

Flavor Twisted Boundary Conditions, Pion Momentum, and the Pion Electromagnetic Form Factor

F.-J. Jiang^{1,2,*} and B. C. Tiburzi^{1,†}

¹*Department of Physics, Duke University,
Box 90305, Durham, NC 27708-0305, USA*

²*Institute for Theoretical Physics, Bern University,
Sidlerstrasse 5, CH-3012 Bern, Switzerland*

(Dated: November 5, 2019)

Abstract

We investigate the utility of partially twisted boundary conditions in lattice calculations of meson observables. For dynamical simulations, we show that the pion dispersion relation is modified by volume effects. In the isospin limit, we demonstrate that the pion electromagnetic form factor can be computed on the lattice at continuous values of the momentum transfer. Furthermore, the finite volume effects are under theoretical control for extraction of the pion charge radius.

PACS numbers: 12.38.Gc, 12.39.Fe

*fjjiang@itp.unibe.ch

†bctiburzi@phy.duke.edu

I. INTRODUCTION

Lattice QCD simulations enable first principles calculation of hadronic properties. Currently, however, observables calculated on the lattice cannot be directly compared with nature due to systematic error. This error arises from approximations used in solving the theory numerically, such as the finite extent of the lattice, the non-vanishing lattice spacing, and larger than physical quark masses. For a large class of observables, effective field theories (EFTs) can be tailored to describe the approximations used in lattice QCD. These EFTs are the reliable tool to remove systematic error in extrapolating data to the physical point, see, e.g. [1]. With growing computational resources and improved numerical algorithms, we are beginning to enter a period in which lattice data in conjunction with EFT methods will enable first principles predictions.

A further limitation encountered in lattice simulations is the available momentum. With periodic boundary conditions, the momentum modes are quantized. On currently available dynamical lattices, the lowest non-vanishing momentum mode is $\sim 500\text{ MeV}$. While EFTs can be tailored to address systematic error in lattice QCD, these low-energy theories cannot be utilized to predict the momentum dependence outside the range of their applicability. The extraction of quantities requiring non-zero momentum, such as phase shifts, electromagnetic moments and radii, is thus limited by coarse grained lattice momentum. Spatially periodic boundary conditions, however, are not mandated. So-called twisted boundary conditions [2, 3, 4, 5, 6, 7, 8, 9, 10, 11] have gained recent attention because they can be utilized to produce continuous hadron momentum [12, 13, 14, 15, 16, 17, 18, 19, 20].

The electromagnetic properties of hadrons paint an intuitive picture of the charge and magnetism distributions of quarks confined in strongly interacting bound states. To resolve such properties of hadrons, one requires momentum transfer and this presents a challenge for the lattice. Calculations of the pion form factor from lattice QCD, for example, have matured since the original pioneering works [21, 22], but still suffer from systematic error. Recently it was demonstrated [23] that current dynamical calculations [24, 25] of the pion charge radii are limited by systematic error relating to the momentum, chiral, and possibly also continuum extrapolations. In this work, we show that the uncertainty surrounding the momentum extrapolation can be eliminated with flavor twisted boundary conditions. With these imposed, one can extract the charge radius from simulations at zero Fourier momentum. As boundary conditions affect the long-range physics on the lattice, we must be careful to address the effects of the finite volume [14]. For partially twisted boundary conditions, we determine the induced isospin splitting and finite volume modification to the pion momentum. Theoretical control over these volume effects is necessary wherever twisted boundary conditions are employed because of the dominance of long-range pion physics in low-energy hadronic observables. Furthermore, we determine the finite volume effects for the extraction of the pion charge radius from lattice simulations with partially twisted boundary conditions.

Our presentation has the following organization. In Section II, we briefly review partially twisted boundary conditions and their incorporation into partially quenched chiral perturbation theory (PQ χ PT). By calculating the pion self-energy, we determine the form of the pion dispersion relation in a finite box and demonstrate that the induced momentum due to twisted boundary conditions is modified by volume effects. The isospin splitting among the pions is also determined in PQ χ PT. Next in Section III, we show that the pion electromagnetic form factor can be determined on the lattice at continuous values of the momentum

transfer. Using PQ χ PT, we then determine the finite volume corrections resulting from partially twisted boundary conditions. These volume effects are a controlled theoretical error that must be removed in order to isolate the pion charge radius from lattice data. Finite volume functions employed in this work are defined in the Appendix. A summary (Section IV) concludes the paper.

II. DISPERSION RELATION WITH TWISTED BOUNDARY CONDITIONS

The quark part of the partially twisted, partially quenched QCD Lagrangian reads

$$\mathcal{L} = \overline{Q} \left(\tilde{D} + m_Q \right) Q, \quad (1)$$

where the six quark fields are accommodated in the vector $Q = (u, d, j, l, \tilde{u}, \tilde{d})^T$, and the mass matrix in the isospin limit of the valence and sea sectors is given by $m_Q = \text{diag}(m_u, m_u, m_j, m_j, m_u, m_u)$. All Q fields satisfy periodic boundary conditions, and the effect of partial twisting has the form of a uniform $U(1)$ gauge field: $\tilde{D}_\mu = D_\mu + iB_\mu$, with the flavor matrix $B_\mu = \text{diag}(B_\mu^u, B_\mu^d, 0, 0, B_\mu^u, B_\mu^d)$. The field B_μ acts as a flavor dependent field momentum: for the u quarks $B_\mu^u = (0, \boldsymbol{\theta}^u/L)$, and similarly for d . The twist angles $\boldsymbol{\theta}$ can be varied continuously and cannot be renormalized by short distance physics. To induce momentum transfer kinematically [16], we will require that at least one component of $\boldsymbol{\theta}^u$ and $\boldsymbol{\theta}^d$ differ.

The dynamical effects due to partial twisting can be addressed by using PQ χ PT in a finite volume and we do so in the p -regime [26]. We construct a periodic coset field Σ coupled to the background gauge field B_μ . In terms of the field Σ , the Lagrangian of PQ χ PT appears as [27, 28, 29, 30, 31]

$$\mathcal{L} = \frac{f^2}{8} \text{str} \left(\tilde{D}_\mu \Sigma \tilde{D}_\mu \Sigma^\dagger \right) - \lambda \text{str} \left(m_Q^\dagger \Sigma + \Sigma^\dagger m_Q \right) + \mu_0^2 \Phi_0^2. \quad (2)$$

With $\mu_0 \rightarrow \infty$, the flavor singlet field $\Phi_0 = \text{str}(\Sigma)/\sqrt{2}$ is integrated out, but the resulting flavor neutral meson propagators have both flavor connected and disconnected (hairpin) contributions. The action of the covariant derivative \tilde{D}^μ is specified by [14]

$$\tilde{D}_\mu \Sigma = \partial_\mu \Sigma + i[B_\mu, \Sigma] + iA_\mu^a [\overline{T}^a, \Sigma], \quad (3)$$

where we have additionally included an isovector source field A_μ^a which will be utilized below in Section III. The block diagonal form of the super-isospin matrices \overline{T}^a is chosen to be $\overline{T}^a = (T^a, 0, T^a)$, where T^a are the usual isospin generators [20]. Expanding \mathcal{L} to tree level, one finds that mesons with quark content $Q\overline{Q}'$ have masses

$$m_{Q\overline{Q}'}^2 = \frac{\lambda}{4f^2} (m_Q + m_{Q'}). \quad (4)$$

We shall often write m_π , and m_{π^0} to denote the mesons formed from purely valence quarks. Other cases for which we also use m_π as an abbreviation will be clarified in the text.

We can use the Lagrangian in Eq. (2) to determine the isospin breaking among the pions in partially twisted PQ χ PT. This was done for completely twisted χ PT in [14], however, additional finite volume terms that ordinarily vanish due to hypercubic invariance were

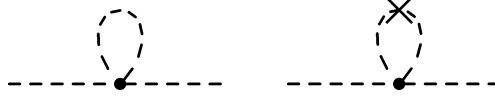


FIG. 1: Pion self-energy diagrams in PQ χ PT. Dashed lines represent mesons, while the cross represents the partially quenched hairpin interaction.

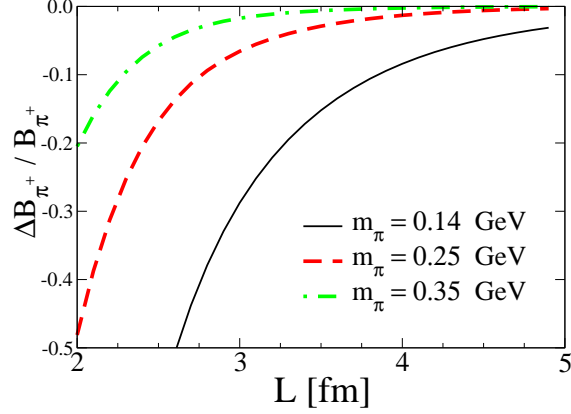


FIG. 2: Maximal change in the induced momentum due to twisting. Here, the pion mass m_π is the valence-sea meson mass, and $\theta^u = -\theta^d$ in the limit of vanishing twist.

overlooked. Evaluating all contributions from the diagrams in Fig. 1, we find that the charged pion dispersion relation has the form

$$E_{\pi^\pm}(\mathbf{p})^2 = (\mathbf{p} + \mathbf{B}_{\pi^\pm} \pm \mathbf{K})^2 + m_\pi^2 + \delta_L(m_{\pi^\pm}^2), \quad (5)$$

where $\delta_L(m_{\pi^\pm}^2)$ is the finite volume shift of the charged pion mass

$$\delta_L(m_{\pi^\pm}^2) = \frac{m_\pi^2}{2f^2} \frac{\partial}{\partial m_\pi^2} [(m_\pi^2 - m_{jj}^2) \mathcal{I}_{1/2}(\mathbf{0}, m_\pi^2)], \quad (6)$$

which happens to be \mathbf{B} -independent at this order, and $\mathcal{I}_\beta(\mathbf{B}, m^2)$ is a finite volume function given in the Appendix. In the dispersion relation, the function \mathbf{K} appears as an additive renormalization to the field momentum $\mathbf{B}_{\pi^\pm} = \pm(\mathbf{B}_u - \mathbf{B}_d)$, and is given by

$$\mathbf{K} = -\frac{1}{f^2} [\mathcal{K}_{1/2}(\mathbf{B}_u, m_{ju}^2) - \mathcal{K}_{1/2}(\mathbf{B}_d, m_{ju}^2)], \quad (7)$$

where $\mathcal{K}_\beta(\mathbf{B}, m^2)$ is another finite volume function defined in the Appendix. The pion field momentum is renormalized only in the directions for which \mathbf{B}_{π^\pm} is non-vanishing. Furthermore, the analogous quenched finite volume contribution vanishes.

We can investigate the finite volume renormalization of the field momentum by considering the relative change in the pion's momentum due to twisting

$$\Delta B_{\pi^+} / B_{\pi^+} = \sum_j K^j / B_{\pi^+}^j. \quad (8)$$

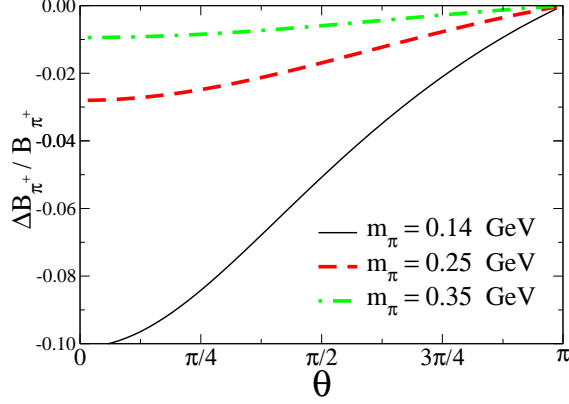


FIG. 3: Relative change in the induced momentum due to twisting as a function of the twist angle. The pion mass m_π refers to the valence-sea meson mass, and the box size is fixed at 2.5 fm .

The relative change in the negatively charged pion's momentum is numerically identical. In the limit $\mathbf{B}_{\pi^+} \rightarrow \mathbf{0}$, we have $\Delta B_{\pi^+}/B_{\pi^+} = \nabla_B \cdot \mathbf{K}$. One should keep in mind, however, that neither of these quantities is accessible without twisted boundary conditions, but the twisted divergence serves as an approximate relative change for small twists. In Fig. 2, we plot the relative change in induced momentum $\Delta B_{\pi^+}/B_{\pi^+}$ in Eq. (8) for the worst case scenario. We take $\boldsymbol{\theta}^u = -\boldsymbol{\theta}^d$ and further choose each component near zero. Finite volume modifications for this case are seen to be substantial from the figure. Thus in applications of twisted boundary conditions, one must take care to avoid large additive volume renormalization of the twisting parameters. Choosing only one flavor to be twisted, e.g. $\boldsymbol{\theta}^d = \mathbf{0}$, and implementing the twist in only one spatial direction reduces the volume effect by a factor of six. Furthermore in the actual implementation of twisted boundary conditions near vanishing twist angles will not be employed. Thus in Fig. 3, we investigate the behavior with respect to the single twist angle θ , where $\boldsymbol{\theta}^u = (0, \theta, 0)$ and $\boldsymbol{\theta}^d = \mathbf{0}$. The relative change in the induced momentum is plotted versus θ for a few valence-sea pion masses (denoted by m_π in the figure), but with the box size $L = 2.5 \text{ fm}$ fixed. The behavior with θ is damped oscillatory and crosses zero when $\theta = (2n + 1)\pi$. For reasonably small values of the twist angle, $\theta \sim \pi/8$, and at (valence-sea) pion masses $\sim 0.3 \text{ GeV}$, the induced momentum is shifted by $\sim 2\%$ from volume effects. Thus the finite volume renormalization of the twist angles can practically be ignored on current lattices. As pion masses are brought down, however, volume renormalization of the induced momentum may need to be accounted for by evaluating Eq. (7).

Aside from finite volume corrections to the mass, the neutral pion dispersion relation is unaffected by twisting. Combining the finite volume shifts for the charged and neutral pions, we find that the isospin splitting due to partially twisted boundary conditions has the form

$$\begin{aligned} \Delta m^2 &= \delta_L(m_{\pi^\pm}^2) - \delta_L(m_{\pi^0}^2) \\ &= \frac{m_\pi^2}{f^2} [\mathcal{I}_{1/2}(\mathbf{0}, m_\pi^2) - \mathcal{I}_{1/2}(\mathbf{B}_{\pi^+}, m_\pi^2)], \end{aligned} \quad (9)$$

and is thus only sensitive to the valence pion mass. In Fig. 4, we plot the relative isospin splitting $\Delta m^2/m_\pi^2$ as a function of the lattice size L for a few values of the valence pion mass m_π . The maximal isospin splitting occurs for $\boldsymbol{\theta}_{\pi^+} = (\pi, \pi, \pi)$, and we have chosen to plot this value to investigate the worst case scenario. From the figure, we see $\sim 10\%$ maximal isospin splitting at the physical pion mass in a relatively small box. For lattice pion masses

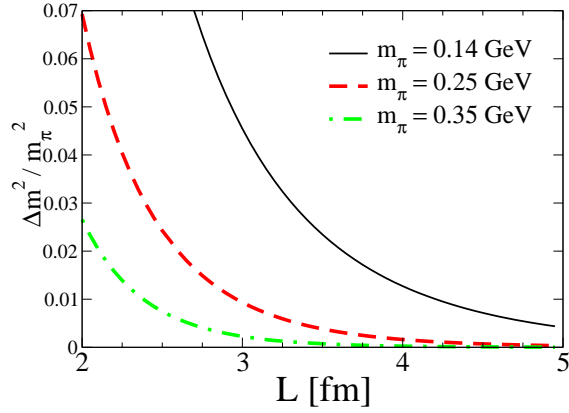


FIG. 4: Maximal isospin splitting between the charged and neutral pions.

$\sim 0.3 \text{ GeV}$, the maximal isospin splitting is $\sim 2\%$ in a 2.5 fm box. For applications of twisted boundary conditions, such as the extraction of the pion charge radius, only one component of θ_{π^+} need be non-vanishing. Moreover, this twist angle should be chosen less than π to reach smaller momentum transfer. These considerations restrict the isospin splitting to be $< 1\%$ for pion masses $\sim 0.3 \text{ GeV}$ in a 2.5 fm box. For this reason we neglect the isospin splitting in virtual loop meson masses below.

Having detailed the finite volume corrections to the pion mass and dispersion relation, we now describe how partially twisted boundary conditions enable the extraction of the pion electromagnetic form factor.

III. PION ELECTROMAGNETIC FORM FACTOR

The pion electromagnetic form factor $G_\pi(q^2)$ arises in the charged pion matrix element of the electromagnetic current J_μ^{em} , namely

$$\langle \pi^+(\mathbf{p}') | J_\mu^{\text{em}} | \pi^+(\mathbf{p}) \rangle = (p' + p)_\mu G_\pi(q^2), \quad (10)$$

with $q = p' - p$. In the isospin limit, however, vector flavor symmetry relates this matrix element to the isospin transition [20]

$$\langle \pi^+(\mathbf{p}') | \bar{u} \gamma_\mu d | \pi^0(\mathbf{p}) \rangle = -\sqrt{2} \langle \pi^+(\mathbf{p}') | J_\mu^{\text{em}} | \pi^+(\mathbf{p}) \rangle, \quad (11)$$

where we have made use of charge conjugation invariance, and the phase convention is that commonly employed in χPT . Thus by calculating the pion form factor from the left-hand side of the above equation, we can induce momentum transfer with partially twisted boundary conditions [16]. The neutral pion is flavor non-singlet and because we work in the isospin limit, the annihilation diagrams contributing to the left-hand side of Eq. (11) exactly cancel. Thus only the contraction shown in Fig. 5 must be calculated. While flavor neutral states in partially twisted (and partially quenched) theories have sicknesses related to lack of unitarity [30, 31], the illness does not infect the states with isospin $I = 1$. Consequently the propagator of the π^0 is diagonal with a simple pole form, and asymptotic π^0 states can be created à la LSZ.

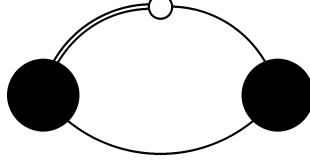


FIG. 5: Contraction for the pion form factor in Eq. (11). The source and sink are denoted by filled circles, the operator insertion by an open circle. Single lines represent twisted d -quark propagators, while the double line represents the twisted u -quark propagator.

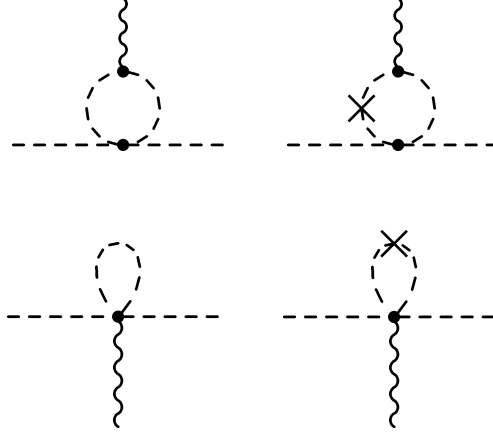


FIG. 6: One-loop contributions to the isospin transition matrix element in PQ χ PT. The wiggly line shows the insertion of the isospin raising operator. Other diagram elements are the same as in Fig. 1.

Application of partially twisted boundary conditions to the matrix element in Eq. (11) thus leads to the kinematical effect

$$\langle \pi^+(\mathbf{0}) | \bar{u} \gamma_4 d | \pi^0(\mathbf{0}) \rangle = -\sqrt{2}(p'_4 + p_4) G_\pi(B^2), \quad (12)$$

where for emphasis we have projected the initial and final states onto zero Fourier momentum, and restricted our attention to the fourth component of the current. The energies are $p_4 = im_\pi$ and $p'_4 = i\sqrt{m_\pi^2 + \mathbf{B}_{\pi+}^2}$, and the momentum transfer squared is $B^2 = 2m_\pi^2(-1 + \sqrt{1 + \mathbf{B}_{\pi+}^2/m_\pi^2})$. The induced three-momentum transfer $\mathbf{B}_{\pi+}$ is given by the difference of twists of the flavors changed $\mathbf{B}_{\pi+} = \mathbf{B}_u - \mathbf{B}_d$. In writing the above expression, we have temporarily ignored dynamical effects from the finite volume. The study in Ref. [20] found considerable volume effects ($\sim 25\%$) in extracting the nucleon isovector magnetic moment at $m_\pi L \approx 4$. To assess the effects of the finite volume on the pion electromagnetic form factor with partially twisted boundary conditions, we must use PQ χ PT and do so in the p -regime.

The one-loop contributions to the isovector form factor are shown in Fig. 6 (along with the requisite wavefunction corrections shown in Fig. 1) and lead to finite volume modifications. In partially twisted PQ χ PT, the isovector current operator also receives a contribution at next-to-leading order from the term

$$\delta J_\mu^+ = i\alpha_9 \tilde{D}_\nu \text{str} \left[\bar{T}^+ \left([\tilde{D}_\mu \Sigma^\dagger, \tilde{D}_\nu \Sigma] - [\tilde{D}_\nu \Sigma^\dagger, \tilde{D}_\mu \Sigma] \right) \right].$$

There are also corrections from the α_4 and α_5 terms of the fourth-order Lagrangian, but these are canceled by wavefunction renormalization. Returning to Eq. (12) but now including the effect of the finite volume at one-loop order in the chiral expansion, we have

$$\langle \pi^+(\mathbf{p}') | \bar{u} \gamma_4 d | \pi^0(\mathbf{p}) \rangle = -\sqrt{2}i \left\{ [E_{\pi^+}(\mathbf{p}') + E_{\pi^0}(\mathbf{p})] [G_\pi(Q^2) + G_{FV}] \right. \\ \left. + [E_{\pi^+}(\mathbf{p}') - E_{\pi^0}(\mathbf{p})] [G_{FV}^{\text{iso}} + (\mathbf{p}' + \mathbf{B}_{\pi^+} + \mathbf{p}) \cdot \mathbf{G}_{FV}^{\text{rot}}] \right\}, \quad (13)$$

where $E_{\pi^+}(\mathbf{p}')$ is given in Eq. (5), and $E_{\pi^0}(\mathbf{p})^2 = \mathbf{p}^2 + m_\pi^2 + \delta_L[m_\pi^2]$. Above Q is the effective momentum transfer, $Q = q + B_{\pi^+}$, and $G_\pi(Q^2)$ is the partially quenched pion electromagnetic form factor in the infinite volume limit [32], namely

$$G_\pi(Q^2) = 1 - \frac{4\alpha_9}{f^2} Q^2 + \frac{1}{48\pi^2 f^2} \left[Q^2 \log \frac{m_{ju}^2}{\mu^2} + 4m_{ju}^2 \mathcal{F} \left(\frac{-Q^2}{4m_{ju}^2} \right) \right]. \quad (14)$$

The auxiliary function $\mathcal{F}(x)$ is defined by

$$\mathcal{F}(x) = (x-1) \sqrt{1 - \frac{1}{x}} \log \frac{\sqrt{1 - \frac{1}{x} + i\varepsilon} - 1}{\sqrt{1 - \frac{1}{x} + i\varepsilon} + 1} + \frac{5}{3}x - 2. \quad (15)$$

The remaining contributions in Eq. (13) are finite volume modifications and have been denoted so with a FV subscript.

The finite volume contribution G_{FV} is the finite volume modification to the form factor. This effect remains even in the absence of twisted boundary conditions. Explicitly we have

$$G_{FV} = \frac{1}{2f^2} \int_0^1 dx \left[\mathcal{I}_{1/2}(x\mathbf{Q} - \mathbf{B}_u, m_{ju}^2 + x(1-x)Q^2) - \mathcal{I}_{1/2}(-\mathbf{B}_u, m_{ju}^2) \right. \\ \left. + \mathcal{I}_{1/2}(x\mathbf{Q} + \mathbf{B}_d, m_{ju}^2 + x(1-x)Q^2) - \mathcal{I}_{1/2}(\mathbf{B}_d, m_{ju}^2) \right], \quad (16)$$

and when $\mathbf{B}_u = \mathbf{B}_d = \mathbf{0}$, we recover finite volume modification to the form factor with periodic boundary conditions [23]. The remaining finite volume effects are due to symmetry breaking introduced by the partially twisted boundary conditions.

The finite volume contribution G_{FV}^{iso} arises from the breaking of isospin and vanishes when $\mathbf{B}_u = \mathbf{B}_d$. This term moreover enters the matrix element proportional to the energy difference between the initial and final states. Ordinarily such an additional structure is forbidden by current conservation. In finite volume, however, the partially twisted boundary conditions break isospin symmetry and the isospin current is no longer conserved. This finite volume correction G_{FV}^{iso} appears as

$$G_{FV}^{\text{iso}} = \frac{1}{6f^2} \int_0^1 dx (1-2x) \left\{ 4\mathcal{I}_{1/2}(x\mathbf{Q}, m_\pi^2 + x(1-x)Q^2) \right. \\ \left. - Q^2 [1 + 2x(1-x)] \mathcal{I}_{3/2}(x\mathbf{Q}, m_\pi^2 + x(1-x)Q^2) \right. \\ \left. + (1-2x)\mathbf{Q} \cdot \boldsymbol{\kappa}_{3/2}(x\mathbf{Q}, m_\pi^2 + x(1-x)Q^2) \right\} - \frac{1}{3} \Delta m^2 / m_\pi^2, \quad (17)$$

and involves the isospin splitting among the pions Δm^2 given in Eq. (9).

The final finite volume modification $\mathbf{G}_{FV}^{\text{rot}}$ arises from the breaking of hypercubic invariance introduced by partially twisted boundary conditions. This contribution is given by

$$\mathbf{G}_{FV}^{\text{rot}} = \frac{1}{4f^2} \int_0^1 dx (1-2x) \left[\mathcal{K}_{3/2}(x\mathbf{Q} - \mathbf{B}_u, m_{ju}^2 + x(1-x)Q^2) + \mathcal{K}_{3/2}(x\mathbf{Q} + \mathbf{B}_d, m_{ju}^2 + x(1-x)Q^2) \right]. \quad (18)$$

Notice this term only vanishes when $\mathbf{B}_u = \mathbf{B}_d = 0$. When $\mathbf{B}_u = \mathbf{B}_d \neq 0$, isospin symmetry is restored and we might expect $\mathbf{G}_{FV}^{\text{rot}}$ to vanish given the way this term enters Eq. (13). This is not the case, however, because twisted boundary conditions break cubic invariance and extra terms are allowed. Indeed the decomposition of the current matrix element in the case when the twisted boundary conditions preserve isospin $\mathbf{B}_u = \mathbf{B}_d \neq 0$,

$$\langle \pi^+(\mathbf{p}') | J_\mu^+ | \pi^0(\mathbf{p}) \rangle = (p' + p)_\mu G(Q^2), \quad (19)$$

relies on $SO(4)$ rotational invariance. While this reduces to hypercubic invariance on the lattice, there are no terms in the EFT that violate $SO(4)$ at this order and the form of Eq. (19) still holds. Twisted boundary conditions, on the other hand, do not respect the hypercubic invariance of the lattice and the above form is no longer valid. The final term $\mathbf{G}_{FV}^{\text{rot}}$ is not invariant under the transformation $Q_j \rightarrow -Q_j$ and thus breaks lattice rotational invariance even in the isospin symmetric case. We should interpret this term in Eq. (13) as arising from cubic symmetry breaking rather than the violation of isospin.¹

Having deduced the volume corrections to the pion form factor using PQχPT, we can now investigate the impact of partially twisted boundary conditions on the extraction of the pion charge radius. To do this, we choose for simplicity $\mathbf{B}^d = \mathbf{0}$ and $\mathbf{B}^u = (0, |\mathbf{B}|, 0)$, with $|\mathbf{B}| = \theta/L$. Furthermore we take the source and sink to be projected onto zero Fourier momentum. We investigate the relative difference of the form factor (minus the isovector charge) in finite volume to infinite volume

$$\delta_L[G_\pi(Q^2) - 1] = \frac{\frac{1}{-\sqrt{2}(p'_4 + p_4)} \langle \pi^+(\mathbf{0}) | J_4^+ | \pi^0(\mathbf{0}) \rangle - G_\pi(Q^2)}{G_\pi(Q^2) - 1}. \quad (20)$$

For small twist angles $\theta \ll 1$, the relative difference in the form factor $\delta_L[G_\pi(Q^2) - 1]$ becomes the relative difference in the charge radius

$$\begin{aligned} \lim_{\theta \rightarrow 0} \delta_L[G_\pi(Q^2) - 1] &\equiv \delta_L[\langle r_\pi^2 \rangle] \\ &= \frac{\langle r_\pi^2 \rangle_L - \langle r_\pi^2 \rangle_\infty}{\langle r_\pi^2 \rangle_\infty}. \end{aligned} \quad (21)$$

Finally as expressions depend on both the valence-valence and valence-sea meson masses, we take the theory to be unquenched, so that $m_{ju}^2 = m_\pi^2$. In Fig. 7, we plot $\delta_L[\langle r_\pi^2 \rangle]$

¹ As for the other finite volume contributions, G_{FV} in Eq. (16) is not invariant under $Q_j \rightarrow -Q_j$ unless $\mathbf{B}_u = \mathbf{B}_d$. The contribution G_{FV}^{iso} is invariant under $Q_j \rightarrow -Q_j$ and so its presence in Eq. (13) is completely due to isospin violation.

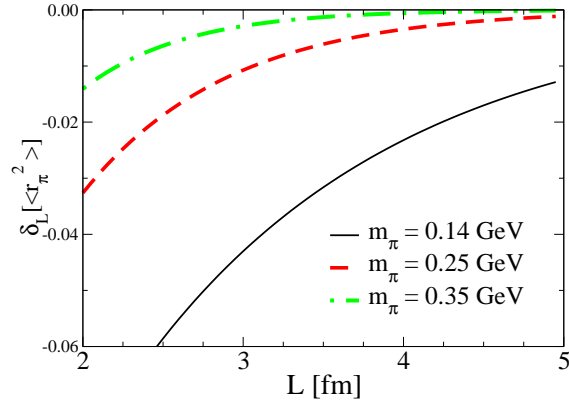


FIG. 7: Finite volume shift of the pion charge radius with partially twisted boundary conditions. Plotted versus the box size L is the relative change in the charge radius $\delta_L[<r_\pi^2>]$ for a few values of the pion mass.

as a function of L for various values of the pion mass to contrast our results with those of Ref. [23]. We plot the total contribution which arises from the three finite volume terms in Eq. (13), however, nearly all of the effect is due to G_{FV} . Contribution from terms that arise from the breaking of symmetries in finite volume, G_{FV}^{iso} and $\mathbf{G}_{FV}^{\text{rot}}$, are suppressed relative to G_{FV} due to the kinematical pre-factor accompanying these terms. The magnitude of the finite volume effect shown in the figure is smaller than that calculated in [23], and has differing sign. In that study, however, periodic boundary conditions were assumed and the extraction of the charge radius required utilizing the smallest available Fourier momentum transfer. With twisted boundary conditions, we have eliminated this restriction. Volume effects are consequently different.

Of course to extract the charge radius from twisted boundary conditions, we require $\theta \neq 0$ and thus investigate $\delta_L[G_\pi(Q^2) - 1]$ in Eq. (20). In Fig. 8, we fix the lattice volume at 2.5 fm and plot the relative difference $\delta_L[G_\pi(Q^2) - 1]$ as a function of θ for a few values of the pion mass. We see that the finite volume effect increases with θ over the range plotted. Generally the finite volume effects for form factors decrease with momentum transfer [20, 33], because as the resolving power of the virtual probe increases, the effect of the finite volume decreases. The behavior with increasing momentum transfer (here parametrized by θ) is indeed damped oscillatory but the oscillations appear beyond the range of the EFT. Nonetheless, the finite volume effect only amounts to a few percent on current dynamical lattices.

Flavor twisted boundary conditions introduce systematic error into the determination of observables, such as the pion charge radius. We stress, however, that this is a controlled effect. There are no extraneous phenomenological form factor fitting functions needed. The EFT can be used for the momentum extrapolation because employing $\theta < \pi$ brings us into the range of applicability of the EFT on current dynamical lattices. Furthermore there are no additional parameters introduced in the EFT to describe the volume dependence with twisted boundary conditions. For mesonic observables, knowledge of the pion decay constant f_π and the pion mass m_π (possibly also the valence-sea pion mass) is enough to remove the volume dependence. Higher-order dependence on the quark mass, volume and momentum transfer can call be calculated systematically in the EFT. In particular, the pion charge radius determined from twisted boundary conditions will be rather insensitive to volume

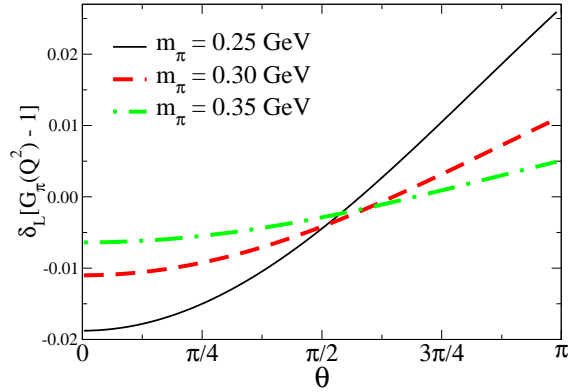


FIG. 8: Finite volume shift of the pion form factor with partially twisted boundary conditions. Plotted versus θ is the relative change in the form factor $\delta_L[G_\pi(Q^2) - 1]$ for a few values of the pion mass. The three-momentum transfer from twisting is $|\mathbf{B}| = \theta \times 0.079 \text{ GeV}$, and the box size is fixed at 2.5 fm .

effects on current dynamical lattices, see Figs. 7 and 8.

IV. SUMMARY

Above we have shown that in the isospin limit the pion electromagnetic form factor may be extracted from the isospin changing matrix element in Eq. (11). Utilizing flavor twisted boundary conditions allows one to circumvent the restriction to quantized momentum transfer. We have detailed the finite volume corrections to the pion mass, dispersion relation, and charge radius using partially twisted PQ χ PT. Addressing these effects is crucial to determining observables, such as the pion charge radius, in simulations with twisted boundary conditions.

We find that the twist angles acquire additive finite volume renormalization which can be sizable near vanishing twist. This effect is only present for dynamical simulations, and the renormalized twist angle $\theta_q^{\text{ren}}(L)$, with $q = u$ or d , is given by

$$\theta_q^{\text{ren}}(L) = \theta_q - \frac{L}{f^2} \mathcal{K}_{1/2} \left(\frac{\theta_q}{L}, m_{jq}^2 \right), \quad (22)$$

where j labels the sea quark (in a two-flavor degenerate sea). For practical applications of partially twisted boundary conditions on current lattices this volume correction is $\sim 2\%$. In finite volume, partially twisted boundary conditions lead to isospin symmetry breaking. The volume induced isospin splitting among the pions is under good theoretical control, $< 1\%$ for practical applications of twisted boundary conditions on current lattices. Finally, the extraction of the pion charge radius with partially twisted boundary conditions introduces no new free parameters, and finite volume effects can be assessed with effective field theory methods. We find that the finite volume effects for extracting the pion charge radius from simulations with twisted boundary conditions are only a few percent.

A simple exercise in isospin algebra [22, 23] shows that the form factors of all isospin $I = 1$ mesons (pseudoscalar, vector, ...) can be computed on the lattice at continuous values of the momentum transfer. Thus, for example, the magnetic moment and electric

quadrupole moment of the ρ^+ meson are accessible at zero Fourier momentum. Apart from the pseudoscalar mesons, the volume effects cannot be calculated systematically, however, as there are no known EFTs for these mesons with a controlled power counting. One would have to demonstrate that the electromagnetic properties extracted from the lattice are stable under changes in the volume. Nonetheless simulating lattice QCD with flavor twisted boundary conditions provides a promising technique to overcome the restriction to quantized momentum transfer.

Acknowledgments

This work is supported in part by the U.S. Dept. of Energy, Grant No. DE-FG02-05ER41368-0 (F.-J.J. and B.C.T.) and by the Schweizerischer Nationalfonds (F.-J.J.).

APPENDIX

Here we define the finite volume functions employed in the main text.

$$\mathcal{I}_\beta(\mathbf{B}, m^2) = \frac{1}{L^3} \sum_{\mathbf{k}} \frac{1}{[(\mathbf{k} + \mathbf{B})^2 + m^2]^\beta} - \int \frac{d\mathbf{k}}{(2\pi)^3} \frac{1}{[(\mathbf{k} + \mathbf{B})^2 + m^2]^\beta}, \quad (23)$$

$$\mathcal{K}_\beta^j(\mathbf{B}, m^2) = \frac{1}{L^3} \sum_{\mathbf{k}} \frac{k^j + B^j}{[(\mathbf{k} + \mathbf{B})^2 + m^2]^\beta}. \quad (24)$$

For each of these finite volume functions, the sum over Fourier momentum modes can be cast into forms that converge exponentially fast by using the Poisson re-summation formula. Resulting expressions are then swiftly evaluated using Jacobi elliptic functions, and/or derivatives thereof, see [14, 20, 23].

-
- [1] C. Bernard et al., Nucl. Phys. Proc. Suppl. **119**, 170 (2003), hep-lat/0209086.
 - [2] D. J. Gross and Y. Kitazawa, Nucl. Phys. **B206**, 440 (1982).
 - [3] A. Roberge and N. Weiss, Nucl. Phys. **B275**, 734 (1986).
 - [4] U. J. Wiese, Nucl. Phys. **B375**, 45 (1992).
 - [5] M. Luscher, S. Sint, R. Sommer, and P. Weisz, Nucl. Phys. **B478**, 365 (1996), hep-lat/9605038.
 - [6] A. Bucarelli, F. Palombi, R. Petronzio, and A. Shindler, Nucl. Phys. **B552**, 379 (1999), hep-lat/9808005.
 - [7] M. Guagnelli et al. (Zeuthen-Rome / ZeRo), Nucl. Phys. **B664**, 276 (2003), hep-lat/0303012.
 - [8] J. Kiskis, R. Narayanan, and H. Neuberger, Phys. Rev. **D66**, 025019 (2002), hep-lat/0203005.
 - [9] J. Kiskis, R. Narayanan, and H. Neuberger, Phys. Lett. **B574**, 65 (2003), hep-lat/0308033.
 - [10] C.-H. Kim and N. H. Christ, Nucl. Phys. Proc. Suppl. **119**, 365 (2003), hep-lat/0210003.
 - [11] C.-H. Kim, Nucl. Phys. Proc. Suppl. **129**, 197 (2004), hep-lat/0311003.
 - [12] P. F. Bedaque, Phys. Lett. **B593**, 82 (2004), nucl-th/0402051.
 - [13] G. M. de Divitiis, R. Petronzio, and N. Tantalo, Phys. Lett. **B595**, 408 (2004), hep-lat/0405002.
 - [14] C. T. Sachrajda and G. Villadoro, Phys. Lett. **B609**, 73 (2005), hep-lat/0411033.

- [15] P. F. Bedaque and J.-W. Chen, Phys. Lett. **B616**, 208 (2005), hep-lat/0412023.
- [16] B. C. Tiburzi, Phys. Lett. **B617**, 40 (2005), hep-lat/0504002.
- [17] J. M. Flynn, A. Juttner, and C. T. Sachrajda (UKQCD), Phys. Lett. **B632**, 313 (2006), hep-lat/0506016.
- [18] D. Guadagnoli, F. Mescia, and S. Simula, Phys. Rev. **D73**, 114504 (2006), hep-lat/0512020.
- [19] G. Aarts, C. Allton, J. Foley, S. Hands, and S. Kim (2006), hep-lat/0607012.
- [20] B. C. Tiburzi, Phys. Lett. **B641**, 342 (2006), hep-lat/0607019.
- [21] G. Martinelli and C. T. Sachrajda, Nucl. Phys. **B306**, 865 (1988).
- [22] T. Draper, R. M. Woloshyn, W. Wilcox, and K.-F. Liu, Nucl. Phys. **B318**, 319 (1989).
- [23] T. B. Bunton, F. J. Jiang, and B. C. Tiburzi, Phys. Rev. **D74**, 034514 (2006), hep-lat/0607001.
- [24] F. D. R. Bonnet, R. G. Edwards, G. T. Fleming, R. Lewis, and D. G. Richards (Lattice Hadron Physics), Phys. Rev. **D72**, 054506 (2005), hep-lat/0411028.
- [25] S. Hashimoto et al. (JLQCD), PoS **LAT2005**, 336 (2006), hep-lat/0510085.
- [26] J. Gasser and H. Leutwyler, Nucl. Phys. **B307**, 763 (1988).
- [27] C. W. Bernard and M. F. L. Golterman, Phys. Rev. **D49**, 486 (1994), hep-lat/9306005.
- [28] S. R. Sharpe, Phys. Rev. **D56**, 7052 (1997), hep-lat/9707018.
- [29] M. F. L. Golterman and K.-C. Leung, Phys. Rev. **D57**, 5703 (1998), hep-lat/9711033.
- [30] S. R. Sharpe and N. Shoresh, Phys. Rev. **D62**, 094503 (2000), hep-lat/0006017.
- [31] S. R. Sharpe and N. Shoresh, Phys. Rev. **D64**, 114510 (2001), hep-lat/0108003.
- [32] D. Arndt and B. C. Tiburzi, Phys. Rev. **D68**, 094501 (2003), hep-lat/0307003.
- [33] W. Detmold and C. J. D. Lin, Phys. Rev. **D71**, 054510 (2005), hep-lat/0501007.